DOI: 10.1002/chem.200600954

Influence of Helical Twisting Power on the Photoswitching Behavior of Chiral Azobenzene Compounds: Applications to High-Performance Switching Devices

Md. Zahangir Alam, Teppei Yoshioka, Tomonari Ogata, Takamasa Nonaka, and Seiji Kurihara*[a]

Abstract: Five photochromic chiral azobenzene compounds and one nonphotochromic chiral compound were synthesized and characterized by IR, ^{1}H NMR spectroscopy, and elemental analysis. Cholesteric liquid crystalline phases were induced by mixing of the nonphotochromic chiral compound and one of the photochromic chiral azobenzene compounds in a host nematic liquid crystal (E44). The helical pitch of the induced cholesteric phase was determined by Cano's wedge method and the helical twisting power (HTP) of each sample was thus determined. The helical twisting powers of azobenzene compounds were decreased upon UV irradiation, due to *trans*→*cis* photoisomerization of azobenzene molecules. Among the azobenzene compounds synthesized in our study, Azo-5, with isomannide (radical) as chiral photochromic dopant, showed the highest HTP and contrast ratio (T_{max}/T_{min}). Photoswitching between compensated nematic phase and cholesteric phase was achieved through reversible *trans*⇄*cis* photoisomerization of the chiral azobenzene molecules through irradiation with UV and visible light, respectively. Transmission rates (contrast ratios) increased with decreasing helical pitch length in the induced cholesteric phase. The influence of helical twisting power on the photoswitching behavior of chiral azobenzene compounds is discussed in detail.

Keywords: chirality · helical structures · liquid crystals · photophysical properties

Introduction

Cholesteric liquid crystals (ChLCs) have attracted the keenest interest of scientists because of their unique helical supramolecular structures, which are capable of selective light reflection in particular spectral regions.[1–3] Chiral photochemical switches are of interest because they can induce the formation of cholesteric phases in nematic hosts, and their helical pitches can be controlled by their photoisomerization.[4] A ChLC can be induced in a nematic liquid crystal (NLC) system through doping with a chiral compound. Cholesteric phases are characterized by the helical packing of the mesogens with a certain sign and a certain pitch. The helical pitch—defined as the distance in a LC needed for the director of the individual mesogens to rotate through a full 360°—is a measure of the chirality of the system. The optical properties of ChLCs depend, in part, on their pitches, and these can be altered either by changing the structures of the liquid crystals themselves or by admixing auxiliaries that change the helical alignments of the molecules of the ChLCs.[5–7] When illuminated with white light, ChLCs reflect light of particular wavelengths dependent on the helical pitch of the LC phase.[8] According to well established theories, the selective reflection wavelength (λ) of a ChLC is governed by Equation (1):

$$\lambda = nP \tag{1}$$

where P is the helical pitch length and n is the refractive index of the liquid crystal.

Another important parameter of molecular design is the so-called helical twisting power (HTP), defined as the ability of a chiral group to induce cholesteric mesomorphism in a nematic host. HTP depends on the dipole–quadrupole interactions of the chiral molecule with its nematogenic neighbors, the anisotropy of the nematic host phase, and on the

[a] Dr. M. Z. Alam, T. Yoshioka, Dr. T. Ogata, Prof. T. Nonaka, Prof. S. Kurihara
Department of Applied Chemistry and Biochemistry
Faculty of Engineering, Kumamoto University
Kurokami 2-39-1, Kumamoto 860-8555 (Japan)
Fax: (+81) 96-342-3679
E-mail: kurihara@gpo.kumamoto-u.ac.jp

order parameter. HTP is related to the helical pitch by Equation (2):[9]

$$\mathrm{HTP} = \frac{1}{P \cdot c} \quad (2)$$

where c is the concentration of the dopant.

When photochromic dopants such as spiropyrans, azobenzenes, and so on are dissolved in a Ch phase, photomodulation of the macroscopic chirality can be induced by the use of suitable light. As the molecular structure is changed by light irradiation, different HTPs are created. Azobenzene molecules undergo reversible *trans*⇄*cis* photoisomerization on irradiation with light of appropriate wavelength, and when an azobenzene is doped into a ChLC, the HTP can be changed by reversible photoisomerization. Thus, as outlined in Equation (2), we can control the helical pitch through reversible photoisomerization.[10]

Many studies on photocontrol of selective reflection of ChLCs have been carried out in recent years. Sackmann showed that selective photoswitching of light reflection, resulting in color changes, can be obtained with a ChLC doped with azobenzene,[11] Witte et al. used a menthone derivative,[12–14] while Shibaev reported a photochromic copolymer of both azobenzene and menthone derivatives.[15–17] In addition, a relationship between molecular structure and HTP of a chiral compound and control of helical structure was reported by Ichimura et al.[18–20] Azobenzene systems represent very attractive phototriggers in Ch media, thanks to their resistance to photofatigue, the simplicity of the molecules, and the ease of modification of their molecular structures.

When a ChLC is placed between two pieces of glass, it forms a parallel texture or a focal conic texture, producing random polydomain structures through surface orientation. LC molecules form homeotropic textures upon application of voltage, turning to a vertical direction adopting an aligned orientation. Our research is aimed at the construction of various light-controllable devices, and we have recently reported the first reversible full-color display device making use of selective reflection by ChLCs.[21]

When a suitable ratio of chiral compounds possessing the ability to produce opposite right and left helical structures and to cancel one another is used, the result is known as a compensated NLC, and does not produce a helical structure.[22] When one component of a chiral system constituting a compensated NLC is a photochromic compound such as an azobenzene, it may be possible to change the state of compensation through a change in the HTP effected by photoisomerization, so that a ChLC with a helical structure may be developed. Previously we have also reported on reversible photoswitching between compensated NLC (transparent state) and ChLC (light-scattering) states of chiral azobenzene molecules.[23]

Since the chirality of a ChLC is sensitive to physical stimuli such as temperature, pressure, and electric field,[24] as well as to chemical modification—including light-induced decomposition, isomerization, and racemization—of the molecules incorporated in the system,[25] ChLCs are significant for optical applications such as Ch displays, optical data recording, photo-optical triggers, polarizers, and reflectors.[26]

In this paper we report the influence of the HTPs of chiral azobenzene compounds on their reversible photoswitching behavior in terms of changes in phase structure and the influence of the orientation state.

Results and Discussion

Properties of compensated nematic LC mixtures: The photochromic chiral azobenzene compounds (Azo-*n*) and the nonphotochromic chiral compound (Menth) used in our experiments are shown in Figure 1, while Figure 2 presents the changes observed in the absorption spectra of Azo-5 in THF during UV irradiation. The UV spectra of Azo-5 showed a strong absorption at around 352 nm, due to a π–π* transi-

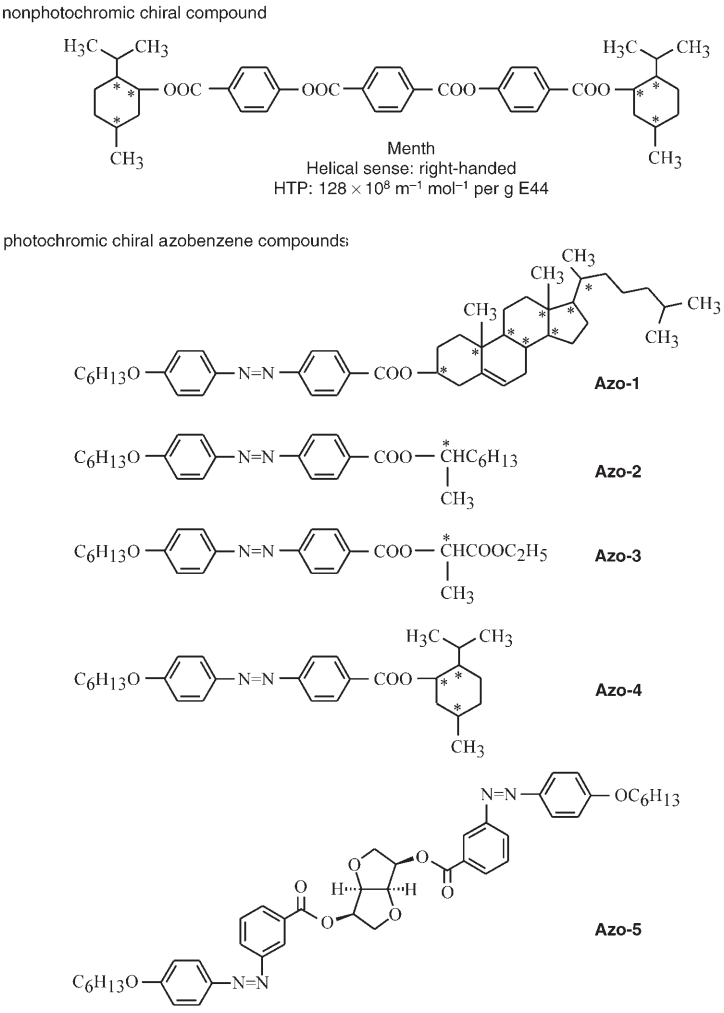

Figure 1. Structures of photochromic and nonphotochromic chiral compounds used in this study.

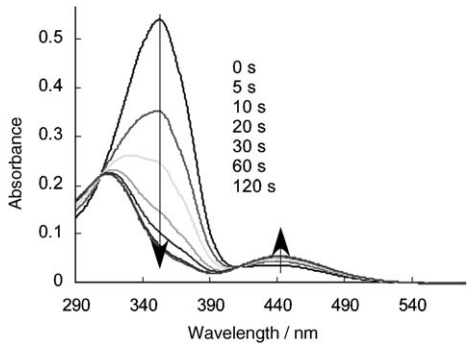

Figure 2. Changes in the absorption spectrum of the chiral photochromic compound Azo-5 in THF on UV irradiation.

tion in the *trans*-azobenzene moiety, with a weak absorption at around 435 nm originating from the n–π* transition. Upon UV irradiation the absorbance at 352 nm is decreased due to *trans*→*cis* photoisomerization while the absorbance at 435 nm is increased a little. A photostationary state is reached after irradiation with UV light for 60 s, while on irradiation with visible light reversible photoisomerization behavior is observed. All the photochromic azo compounds displayed similar reversible photoisomerization behavior on irradiation with UV and visible light.

A Ch phase was induced by mixing each chiral azobenzene compound and the nonphotochromic chiral compound in the host nematic liquid crystal (E44). The helical sense (helical rotatory direction) of the induced cholesteric liquid crystal was affected by the chirality of each chiral substituent: all the chiral azobenzene compounds produced left-handed helixes, while a right-handed helix was obtained from chiral Menth. The helical pitch of each chiral azobenzene compound (Azo-*n*) and Menth compound were determined by Cano's wedge method[27] and the HTP was calculated in each case by use of Equation (2). The HTPs of the chiral azobenzene compounds (Azo-*n*) are summarized in Table 1, while the HTP of the Menth compound was $128\times10^{8}\,m^{-1}\,mol^{-1}$ per g E44. The HTPs of the azobenzene compounds after UV irradiation are also shown in Table 1: all were decreased upon UV irradiation, as a result of photoisomerization of the azobenzene compounds from their *trans* to their *cis* forms on UV irradiation. These results suggest that the strengths of the HTPs and the changes in HTPs (ΔHTP in Table 1) of the azobenzene compounds before and after irradiation depend on the molecular structure of each chiral substituent.

Compensated NLC samples were prepared on the basis of the calculated HTP values, by mixing the chiral azobenzene compounds and the nonphotochromic chiral compound in E44. The ratios (E44/Menth/Azo-*n*) and phase transition temperatures of those samples are shown in Table 2, the proportion of E44 as host NLC in this study being 80 weight-percent. A Schlieren texture corresponding to a NLC was confirmed in all samples by polarized optical microscopic observations, and upon UV irradiation these compensated NLC samples were converted into Ch phases with helical structures. Fingerprint textures observed by polarized optical microscopy confirmed the formation of ChLC state.

Table 2. Phase transition temperatures of (E44/Chiral/Azo-*n*) mixtures observed during cooling.

Azo-*n*	(E44/Chiral/Azo-n) [wt.%]	Phase transition temperature [°C]
Azo-1	80:1.5:18.5	N 85 I
Azo-2	80:4.4:15.6	N 82 I
Azo-3	80:6.3:13.7	N 82 I
Azo-4	80:7.2:12.8	N 79 I
Azo-5	80:9.8:10.2	N 84 I

N = Nematic phase. I = Isotropic phase.

Figure 3 shows polarizing microscope photographs of an induction process with the sample (E44/Chiral/Azo-2 80:9.8:10.2 wt%) changing to a Ch phase from a compensated N phase on UV irradiation. In the initial state the opposite helical senses of the Azo-2 and the Menth each compensated the other's HTP. Consequently, a Schlieren texture indicating the N phase was observed (left-hand photograph).

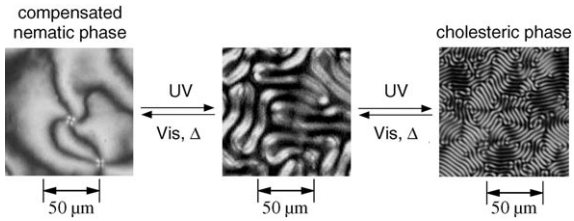

Figure 3. Reversible photochemical phase transition between a compensated nematic phase and a cholesteric phase (E44/Chiral/Azo-2 80:9.8:10.2 wt%) on UV and visible light irradiation.

Table 1. Helical twisting powers and helical pitch lengths of cholesteric LCs induced by UV irradiation, together with contrast ratios (T_{max}/T_{min}) calculated from the differences in transmittance by UV and visible light irradiation at 25 °C.

Spectrum	Azo-*n*	HTP [$\times10^{8}\,m^{-1}\,mol^{-1}$ per g E44] Before irradiation	After irradiation	ΔHTP [%]	Helical pitch [μm]	T_{min} [%]	T_{max}/T_{min}
1	Azo-1	10.7	10.5	−2	30.1	89	1.0
2	Azo-2	32.0	20.9	−35	4.82	45	2.0
3	Azo-3	36.6	19.9	−46	2.23	27	3.3
4	Azo-4	49.0	10.8	−78	1.23	21	4.2
5	Azo-5	129	20.5	−84	0.69	16	5.6

The compensated N state is destroyed upon UV irradiation because of the photochemical decrease in the HTP of Azo-2, with a right-handed Ch phase based on Menth developing and the fingerprint texture confirming the formation of a Ch phase (right-hand photograph). In addition, Figure 3 also indicates

that the helical pitch decreased with UV irradiation. Reversible photoisomerization from the *cis* to the *trans* form was observed on visible light irradiation, and the HTP was now compensated once more, so the compensated N phase was recovered again on visible light irradiation.

Photoswitching behavior: Each sample was injected into a 5 μm homeotropic and homogeneous glass cell by capillary force. Figure 4 shows a schematic diagram illustrating the measurement of the photochemical switching behavior of chiral azobenzene compounds, determined under irradiation with UV and visible light. To investigate the influence of the orientation of the cell on photoswitching behavior, two types of cell—homeotropic and homogeneous glass cells—were used. Figure 5a shows the results obtained with a homeotropic glass cell. In the initial state (before UV irradiation), all samples were in a compensated nematic phase and showed about a 90% transmission rate, forming a homeotropic structure. On UV and visible light irradiation, however, all samples except for Azo-1 (Azo-1 did not show photoswitching behavior at all, and the transmission rate was constant in the vicinity of 90%) showed photoswitching behavior. The photoswitching rates also differed for different samples. Table 1 shows HTP and ΔHTP values for each azobenzene compound, helical pitches (determined by Cano's wedge method) of the Ch phases induced by UV light irradiation, and contrast ratios (T_{max}/T_{min}) calculated from the maxima and the minima of the transmission rates in Figure 5. The results shown in Table 1 revealed that samples with lower helical pitches showed higher contrast ratios or, in other words, that a shorter helical pitch produces a focal conic texture with high density and indicates a strong light-scattering state. Therefore, it is not only the strength of HTP but also the quantity of change in HTP (ΔHTP) that is important for photoswitching behavior, due to the difference in phase structures. It is believed that the ΔHTP values had a large influence on photoswitching speed and the transmission rate; that is, the contrast ratios of the chiral azobenzene compounds.

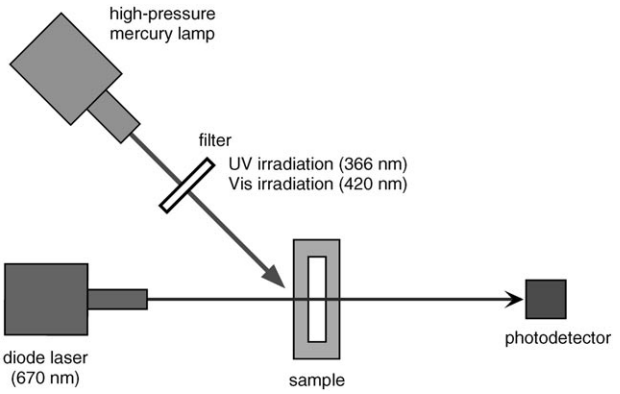

Figure 4. Experimental setup for measuring photochemical switching behavior.

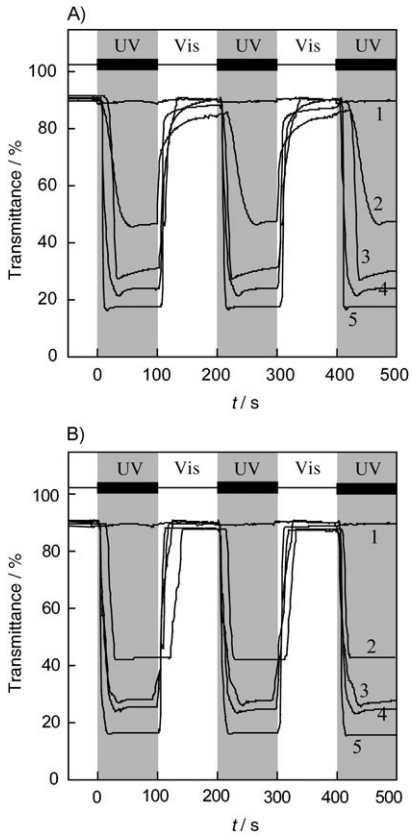

Figure 5. Changes in the intensity of light transmitted from a diode laser (670 nm, 3.8 mW cm^{-2}) through mixtures of E44, chiral, and Azo-*n* (80/*x*/20−*x* wt%) in a 5 μm homeotropic glass cell (A) and a homogeneous glass cell (B) on UV (3.2 mW cm^{-2}) and visible (8.3 mW cm^{-2}) light irradiation at 25°C. 1: Azo-1. 2: Azo-2. 3: Azo-3. 4: Azo-4. 5: Azo-5.

Figure 6 shows transmission spectra of the sample (E44/Chiral/Azo-5 80:9.8:10.2 wt%) in the transparent state and in the light-scattering state. In the initial state the transmission rate was as high as about 80%, and from Figure 6 it can also be seen that there was no wavelength dependence in the region above 500 nm, but that the transmission rates

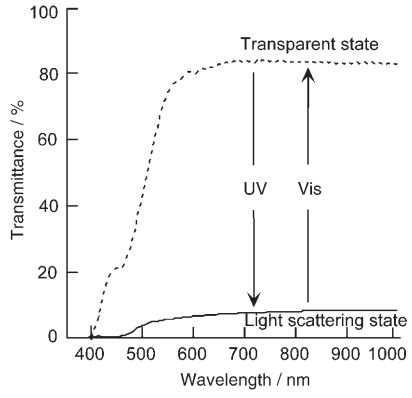

Figure 6. Transmittance spectra of a mixture of E44, chiral, and Azo-5 (80/9.8/10.2 wt%) before (dotted line) and after (solid line) UV light irradiation for 30 s at 25°C.

at 500 nm or less were decreased both in the initial (transparent) state and in the light-scattering (opaque) state because of the accumulation of absorption wavelengths of the azobenzene chromophores in that region. From the above, it is believed that there is potential to intercept light of a wide wavelength range, including in the visible domain, in the light-scattering state of the sample in this study. The results of photoswitching in a homogeneous glass cell were similar to those obtained with the homeotropic glass cell, as shown in Figure 5b. In the homogeneous glass cell, compensated NLCs formed a parallel texture and the sample consequently became transparent. Upon UV irradiation the transmission rate was decreased and the transparent state was converted into to an opaque one (light-scattering state).

We investigated the effect of UV light intensity on transmittance of the sample (E44/Chiral/Azo-5 80:9.8:10.2 wt%) in the light-scattering state in homeotropic and homogeneous glass cells to elucidate the outbreak mechanism of the light-scattering state. Figure 7 shows the transmission rate of the (E44/Chiral/Azo-5) sample as a function of irradiation time with different power intensities of UV light. The strength of the UV irradiation was 0.4, 1.0, 1.5, and 3.2 mW cm^{-2}. In the case of the homeotropic cell the photoisomerization rate became slower with decreasing intensity of UV irradiation, as shown in Figure 7a, with the transmission of the light-scattering state finally reaching a constant value regardless of the intensity of UV irradiation. Because the Ch phase always forms a focal conic texture in the homeotropic glass cell, this means that the Ch phase can form the same light-scattering state regardless of the progress of photoisomerization (Figure 8). On the other hand, in the case of the homogeneous glass cell, the transmission rate was found to be strongly dependent on the intensity of the irradiating UV light. It is assumed that this is due to the influence of the orientation power of the homogeneous glass cell. The Ch phase tends to produce a planar structure in the homogeneous glass cell, and consequently shows selective reflection properties. However, it is thought that the influence of orientation power of a cell becomes low when the phase structure changes instantly (Figure 8). Therefore, the transmittance obtained under illumination with high-intensity light was extremely low and was found to be dependent on the light intensity.

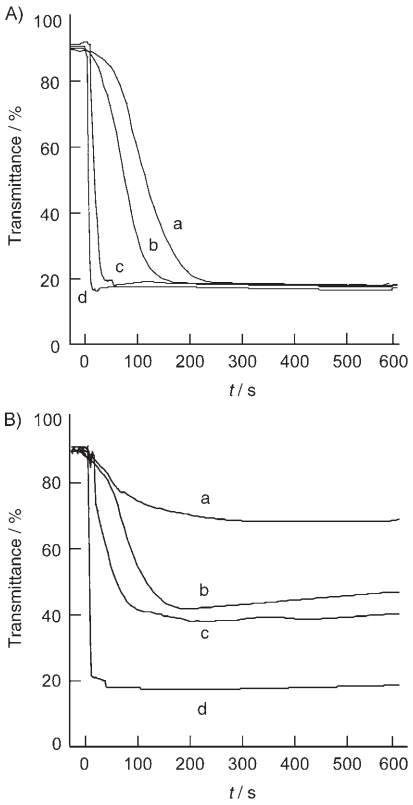

Figure 7. Changes in the intensity of transmitted light from a diode laser (670 nm, 3.8 mW cm^{-2}) through an (E44/Chiral/Azo-5 80:9.8:10.2 wt%) mixture in a 5 μm homeotropic glass cell (A) and in a homogeneous glass cell (B) under UV light irradiation of various intensities at 25°C. a) 0.4 mW cm^{-2}. b) 1.0 mW cm^{-2}. c) 1.5 mW cm^{-2}. d) 3.2 mW cm^{-2}.

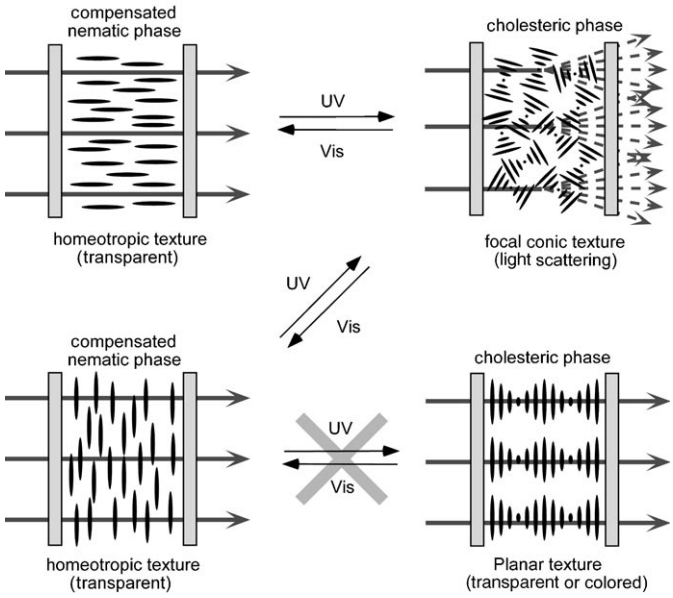

Figure 8. Schematic representation of reversible photoswitching between transparent and opaque state.

The contrast ratios of the chiral azobenzene compounds calculated from the differences in transmittance caused by UV and visible light irradiation with an intensity of 3.2 mW cm^{-2} at 25°C in homeotropic and homogeneous glass cells are summarized in Table 3. These values do not show any significant differences. From Table 1 it is evident that the helical pitch length of the Ch phase influences the contrast ratio calculated from the difference in transmittance caused by UV and visible light irradiation, the contrast ratio increasing with decreasing helical pitch length. Both helical pitch length and helical twisting power thus influenced the photoswitching behavior of chiral azobenzene compounds.

Table 3. Contrast ratios of chiral azobenzene compounds calculated from the differences in transmittance induced by UV and by visible light (3.2 mW cm^{-2}) irradiation in a homeotropic or a homogeneous glass cell at 25 °C.

Spectrum No.	Azo-*n*	Homeotropic glass cell		Homogeneous glass cell	
		T_{min} [%]	T_{max}/T_{min}	T_{min} [%]	T_{max}/T_{min}
1	Azo-1	89	1.0	89	1.0
2	Azo-2	45	2.0	42	2.1
3	Azo-3	27	3.3	27	3.4
4	Azo-4	21	4.2	24	3.8
5	Azo-5	16	5.6	17	5.4

Application of these chiral azobenzene compounds to high-efficiency photoswitching devices: The objective of our research is to improve the performance of photoswitching, enabling application to various optical devices. To investigate the photoswitching behavior of the chiral azobenzene compounds, the influence of the compositions of the ChLC mixtures on photoisomerization rates—that is, transmission rates—was investigated. The data given in Table 4 show that the helical pitches of ChLCs could be changed by varying their compositions: the helical pitches of the ChLCs decreased with increases in the concentrations of the chiral dopant and the photochromic chiral azobenzene compounds. Table 4 shows the changes in the helical pitches and contrast ratios of (E44/Chiral/Azo-5) ChLC systems with changes in composition. Azo-5 was chosen for these experiments because of its high ΔHTP value. The changes in the transmitted light intensity of a diode laser (670 nm) through (E44/Chiral/Azo-5) mixtures in a 25 μm homogeneous glass on UV and visible light irradiation at 25 °C are presented in Figure 9. The contrast ratios of the ChLC systems increased with increasing concentration of the chiral dopant and photochromic chiral azobenzene compounds, while the transmission rates of the light-scattering states of the ChLCs with lower helical pitch decreased to 2% and the contrast ratios increased to about 40%, the focal conic texture becoming denser and the transmission rate decreasing as a consequence. Photoswitching with high contrast ratios is thus possible with these photochromic chiral azobenzene compounds.

Table 4. Phase transition temperatures during cooling, helical pitch lengths induced by UV irradiation, and contrast ratios (T_{max}/T_{min}) of (E44/Chiral/Azo-5) mixtures.

E44/Chiral/Azo-5 [wt.%]	Phase transition temperature [°C]	Helical pitch [μm]	T_{min} [%]	T_{max}/T_{min}
80:9.8:10.2	N 84 I	0.69	3.0	30.3
75:12.3:12.7	N 76 I	0.47	2.4	37.9
70:14.8:15.2	N 70 I	0.33	2.3	39.6

N = Nematic phase. I = Isotropic phase

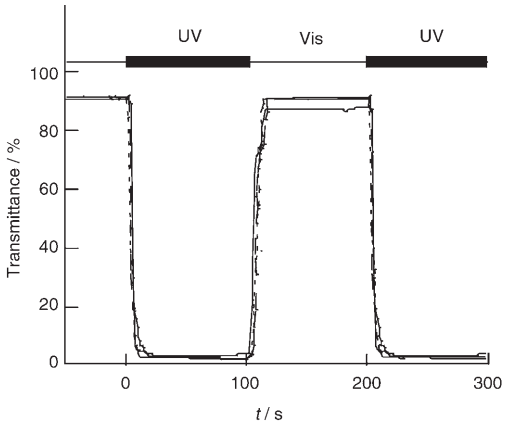

Figure 9. Changes in diode laser (670 nm) transmittance through (E44/Chiral/Azo-5) mixtures in a homogeneous glass cell on UV (3.2 mW cm^{-2}) and visible light (8.3 mW cm^{-2}) irradiation at 25 °C. Compositions of (E44/Chiral/Azo-5) mixtures are: 80:9.8:10.2 wt% (——), 75:12.3:12.7 wt% (-----), and 70:14.8:15.2 wt% (– – –).

Conclusion

Compensated N phases were induced by mixing of a non-photochromic chiral compound (Menth) and photochromic chiral azobenzene compounds (Azo-*n*) with a low molecular weight host LC (E44) in the ratios that compensated one another's HTP. Reversible phase transformation between the compensated N phase (transparent state) and the Ch phase (opaque state) was achieved by means of reversible photoisomerization under UV and visible light irradiation, respectively. The photoswitching times and transmission rates (contrast ratios) of the chiral azobenzene compounds under UV and visible light irradiation conditions were found to be related to the quantity of change in HTP on photoisomerization. Contrast ratios (T_{max}/T_{min}) increased with decreasing helical pitch length of the induced cholesteric phases. In the case of the homogeneous glass cell, LC molecules were easily influenced by the orientation of the cell. The light-scattering state of a sample had the potential to intercept light of all of the visible domain, and consequently a high efficiency of photoswitching was possible, together with a high contrast ratio. The results of this study are very significant in terms of application of the photoswitching behavior of the chiral azobenzene compounds to various photodevices.

Experimental Section

Synthesis of photochromic and nonphotochromic chiral compounds: Photochromic chiral azobenzene compounds Azo-1 to Azo-4 were synthesized by diazo coupling between 4-aminobenzoic acid and phenol to give 4-(4-hydroxyphenylazo)benzoic acid. Azo-5 was synthesized by diazo coupling between 3-aminobenzoic acid and phenol to give 3-(4-hydroxyphenylazo)benzoic acid. After etherification with hexyl bromide, esterification with suitable chiral alcohols was carried out in the presence of dicyclohexylcarbodiimide (DCC) in dichloromethane and the product was purified by column chromatography (silica gel, $CHCl_3$ as eluent) and re-

crystallization from ethanol. The following alcohols were used to synthesize the corresponding chiral azobenzene compounds: cholesterol for Azo-1, (*S*)-(+)-octanol for Azo-2, ethyl (*S*)-(−)-lactate for Azo-3, (1*R*,2*S*,5*R*)-(−)-menthol for Azo-4, and isomannide for Azo-5.

Menth: The nonphotochromic chiral compound (Menth) was synthesized as follows. 4-Hydroxybenzoic acid was treated with 3,4-dihydro-2*H*-pyran for protection of the hydroxy group and then with (1*S*,2*R*,5*S*)-(+)-menthol in the presence of DCC in dichloromethane to give 1-menthyl 4-(tetrahydropyran-2-yloxy)benzoate. This benzoate derivative was heated at 60 °C in ethanol for 4 h in the presence of pyridinium *p*-toluenesulfonate to yield 2-menthyl 4-hydroxybenzoate, and this benzoate derivative was condensed with terephthalic acid in dichloromethane in the presence of DCC to yield the crude chiral compound, which was purified by column chromatography (silica gel, $CHCl_3$ as eluent) and recrystallized from ethanol.

E44: Low molecular weight nonchiral nematic LC, purchased from Merck Co. Ltd., used as received.

The synthesized compounds were characterized by elemental analysis and by IR and ^{1}H NMR spectroscopy. The characterization data of the compounds are as follows.

Azo-1: ^{1}H NMR ($CDCl_3$): δ = 0.8–2.2 (m, 29H; methylene), 4.1 (t, 2H; $ArOCH_2$-), 5.0 (m, 1H; COOCH-), 7.0–8.2 ppm (m, 8H; aromatic); IR: $\tilde{\nu}$ = 1604 (aromatic), 1710 cm^{-1} (C=O); elemental analysis calcd (%) for $C_{29}H_{40}N_2O_3$: C 75.0, H 8.62, N 6.03; found: C 74.7, H 8.58, N 6.15.

Azo-2: ^{1}H NMR ($CDCl_3$): δ = 0.7–1.8 (m, 27H; methylene), 4.0 (t, 2H; $ArOCH_2$-), 5.0 (m, 1H; COOCH-), 7.0–8.2 ppm (m, 8H; aromatic); IR: $\tilde{\nu}$ = 1600 (aromatic), 1709 cm^{-1} (C=O); elemental analysis calcd (%) for $C_{27}H_{38}N_2O_3$: C 73.9, H 8.73, N 6.39; found: C 73.8, H 8.63, N 6.63.

Azo-3: ^{1}H NMR ($CDCl_3$): δ = 0.9, 1.6 (m, 6H; methyl), 1.2–1.8 (m, 11H; methylene), 4.0 (t, 2H; $ArOCH_2$-), 4.2 (t, 2H; $COOCH_2$-), 5.3 (m, 1H; COOCH-), 7.0–8.2 ppm (m, 8H; aromatic); IR: $\tilde{\nu}$ = 1601 (aromatic), 1716, 1725 cm^{-1} (C=O); elemental analysis calcd (%) for $C_{24}H_{30}N_2O_3$: C 67.6, H 7.09, N 6.57; found: C 67.5, H 7.00, N 6.68.

Azo-4: ^{1}H NMR ($CDCl_3$): δ = 0.8–2.2 (m, 29H; methylene), 4.1 (t, 2H; $ArOCH_2$-), 5.0 (m, 1H; COOCH-), 7.0–8.2 ppm (m, 8H; aromatic); IR: $\tilde{\nu}$ = 1604 (aromatic), 1710 cm^{-1} (C=O); elemental analysis calcd for $C_{29}H_{40}N_2O_3$: C 75.0, H 8.62, N 6.03; found: C 74.7, H 8.58, N 6.15.

Azo-5: ^{1}H NMR ($CDCl_3$): δ = 1.3–1.8 (m, 16H; methylene), 4.0 (t, 4H; $ArOCH_2$-), 5.4 (m, 2H; COOCH-), 7.0–8.6 ppm (m, 16H; aromatic); IR: $\tilde{\nu}$ = 1598 (aromatic), 1721 cm^{-1} (C=O); elemental analysis calcd (%) for $C_{44}H_{50}N_4O_8$: C 69.3, H 6.61, N 7.34; found: C 69.3, H 6.59, N 7.34.

Nonphotochromic chiral compound (Menth): ^{1}H NMR ($CDCl_3$): δ = 0.8–2.2 (m, 36H; methylene), 5.0 (m, 2H; COOCH-), 7.3–8.4 ppm (m, 12H; aromatic); IR: $\tilde{\nu}$ = 1064 (aromatic), 1708 cm^{-1} (C=O); elemental analysis calcd (%) for $C_{42}H_{50}O_8$: C 73.9, H 7.38; found: C 73.8, H 7.39.

Characterization of azobenzene compounds and liquid crystal mixtures: LC mixtures were prepared by addition of one of the azobenzene compounds (Azo-*n*) and/or a nonphotochromic chiral compound (Menth) to the host nematic LC (E44). The thermal phase transition behavior of the synthesized compounds and their LC mixtures was examined by polarizing optical microscopic observation (POM, Olympus BHSP polarizing optical microscope; Mettler FP80 and FP82 hot stage and controller).

Preparation of compensated nematic LC mixtures: Compensated nematic LC mixtures were prepared by mixing the nonphotochromic chiral compound and a photochromic chiral azobenzene compound in E44 in the ratio that compensated the other's HTP. The LC mixtures were injected into a 5 μm glass cell with homogeneous or homeotropic alignment (EHC Co., Ltd.) by capillary force.

Photoresponsive properties: While the sample was irradiated the change in the helical structure was explored by monitoring of transmitted light intensity through the samples with a diode laser (Suruga Seiki Co.; 670 nm; 3 mW cm^{-2}). The photoirradiation was carried out with a 500 W high-pressure Hg lamp (Ushio) fitted with a glass filter: UTVAF-35 (Sigma Koki Co.) for ultraviolet (UV) irradiation (366 nm) or SCF-42L (Sigma Koki Co.) for visible light irradiation (436 nm).

Helical pitch measurement: The helical pitch of each induced cholesteric phase was determined by the Cano wedge method.[27] Experiments for determining helical pitch were performed with injected samples in a wedge cell (EHC, Japan).

[1] B. L. Feringa, R. A. van Delden, N. Koumura, E. M. Geertsema, *Chem. Rev.* **2000**, *100*, 1789.
[2] *Handbook of Liquid Crystals, Vol. 1* (Eds.: D. Demus, J. Goodby, G. W. Gray, H.-W. Spiess, V. Vill), Wiley-VCH, Weinheim **1998**.
[3] M. Schadt, *Liq. Cryst.* **1993**, *14*, 73.
[4] a) D. Dunmar, K. Toniyama, *Handbook of Liquid Crystals, Vol. 1*, Wiley-VCS, Weinheim **1998**, pp. 215–239; b) G. Meier, in *Applications of Liquid Crystals*, Springer, Berlin, Heidelberg, New York **1975**, pp. 1–21; c) S. Chandrasekhar, *Liquid Crystals*, Cambridge University Press, Cambridge, UK **1977**.
[5] G. Gottarelli, M. Hibert, B. Samori, G. Solladie, G. Spada, R. Zimmerman, *J. Am. Chem. Soc.* **1983**, *105*, 7318.
[6] G. Gottarelli, G. Spada, *Mol. Cryst. Liq. Cryst.* **1985**, *123*, 377.
[7] G. Gottarelli, B. Samorei, *Tetrahedron* **1981**, *37*, 395.
[8] D.-K. Yang, X.-Y. Huang, Y.-M. Zhu, *Annu. Rev. Mater. Sci.* **1997**, *27*.
[9] P. G. de Gennes, J. Prost, *The Physics of Liquid Crystals*, Oxford Science Publications, **1993**.
[10] *Photochromism, Techniques of Chemistry, Vol. 3* (Ed.: G. H. Brown), Wiley-Interscience, **1971**.
[11] E. Sackmann, *J. Am. Chem. Soc.* **1971**, *93*, 25.
[12] P. van de Witte, M. Brehmer, J. Lub, *Adv. Mater.* **1998**, *10*, 17.
[13] P. van de Witte, M. Brehmer, J. Lub, *J. Mater. Chem.* **1999**, *9*, 9.
[14] P. van de Witte, J. Lub, *Liq. Cryst.* **1998**, *24*, 6.
[15] A. Y. Bobrovsky, N. I. Boiko, V. P. Shibaev, *Liq. Cryst.*.**1998**, *24*, 5.
[16] A. Y. Bobrovsky, N. I. Boiko, V. P. Shibaev, J. Springer, *Adv. Mater.* **2000**, *12*, 16.
[17] A. Y. Bobrovsky, V. P. Shibaev, *Adv. Funct. Mater.* **2002**, *12*, 5.
[18] C. Ruslim, K. Ichimura, *Adv. Mater.* **2001**, *13*, 1.
[19] C. Ruslim, K. Ichimura, *Adv. Mater.* **2001**, *13*, 9.
[20] C. Ruslim, K. Ichimura, *J. Phys. Chem. B* **2000**, *104*, 17.
[21] T. Yoshioka, T. Ogata, T Nonaka, M. Moritsugu, S. N. Kim, S. Kurihara, *Adv. Mater.* **2005**, *17*.
[22] E. Sackmann, *J. Am. Chem. Soc.* **1968**, *90*, 13.
[23] S. Kurihara, S. Nomiyama, T. Nonaka, *Chem. Mater.* **2001**, *13*, 6.
[24] H. Coles, in *Handbook of Liquid Crystals, Vol. 2A* (Eds.: D. Demus, J. Goodby, G. W. Gray, W.-H. Spiess, V. Vill), Wiley-VCH, Weinheim, **1998**, Chapter 4, p. 382.
[25] a) G. Solladié, R. G Zimmermann, *Angew. Chem.* **1985**, *97*, 70; *Angew. Chem. Int. Ed. Engl.* **1985**, *24*, 64; b) R. P. Lemieux, G. B. Schuster, *J. Org. Chem.* **1993**, *58*, 100; c) G. Heppke, H. Marschal, P. Nürnberg, F. Oestreicher, G. Scherowsky, *Chem. Ber.* **1981**, *114*, 2501; d) A. Y. Bobrovsky, N. I. Boiko, V. P. Shibaev, *Liq. Cryst.* **1998**, *25*, 79; e) N. P. M. Huck, W. F. Jangr, B. de Lange, B. L. Feringa, *Science* **1996**, *273*, 1686.
[26] a) D. J. Dyer, U. P. Schöder, K. P. Chang, R. J. Twieg, *Chem. Mater.* **1997**, *9*, 1665; b) N. Tamaoki, A. V. Parfenov, A. Masaki, H. Matsuda, *Adv. Mater.* **1997**, *9*, 1102; c) N. Tamaoki, S. Song, M. Moriyama, H. Matsuda, *Adv. Mater.* **2000**, *12*, 94; d) R. A. M. Hikmet, H. Kemperman, *Nature*, **1998**, *392*, 476; e) P. van de Vitte, E. E. Neuteboom, M. Brehmer, J. Lub, *J. Appl. Phys.* **1999**, *85*, 7517; f) B. L. Feringa, N. P. Huck, H. A. van Doren, *J. Am. Chem. Soc.* **1995**, *117*, 9929; g) C. Denekamp, B. L. Feringa, *Adv. Mater.* **1998**, *10*, 1080.
[27] G. Solladie, R. G. Zimmermann, *Angew. Chem.* **1984**, 96, 335; *Angew. Chem. Int. Ed. Engl.* **1984**, 23, 348.

Received: July 4, 2006
Revised: October 11, 2006
Published online: January 3, 2007

